

# In Vivo Evaluation of the Pulmonary Toxicity of Cellulose Nanocrystals: A Renewable and Sustainable Nanomaterial of the Future

Naveena Yanamala,<sup>†</sup> Mariana T. Farcas,<sup>†</sup> Meghan K. Hatfield,<sup>†</sup> Elena R. Kisin,<sup>†</sup> Valerian E. Kagan,<sup>§</sup> Charles L. Geraci,<sup>||</sup> and Anna A. Shvedova<sup>\*,†,‡</sup>

<sup>†</sup>Pathology and Physiology Research Branch/NIOSH/CDC, Morgantown, West Virginia 26505, United States

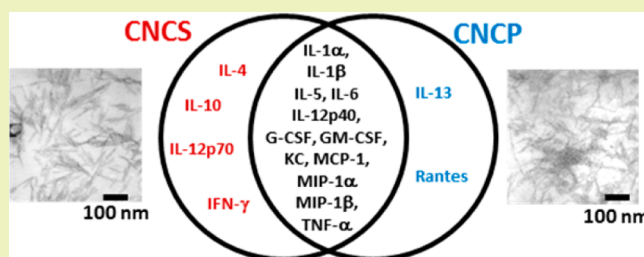
<sup>‡</sup>Department of Physiology and Pharmacology, West Virginia University, Morgantown, West Virginia 26505, United States

<sup>§</sup>Department of Environmental and Occupational Health, University of Pittsburgh, Pittsburgh, Pennsylvania 15260, United States

<sup>||</sup>Education and Information Division, National Institute for Occupational Safety and Health, Cincinnati, Ohio 45226, United States

**ABSTRACT:** The use of cellulose as building blocks for the development of novel functional materials is rapidly growing. Cellulose nanocrystals (CNC), with advantageous chemical and mechanical properties, have gained prominence in a number of applications, such as in nanofillers in polymer composites, building materials, cosmetics, food, and the drug industry. Therefore, it becomes critical to evaluate the potential health effects associated with CNC exposures. The objective of this study was to compare pulmonary outcomes caused by exposure of C57BL/6 mice to two different processed forms of CNC derived from wood, i.e., CNCS (10 wt %; gel/suspension) and CNCP (powder), and compare to asbestos induced responses. Pharyngeal aspiration with CNCS and CNCP was found to facilitate innate inflammatory response assessed by an increase in leukocytes and eosinophils recovered by bronchoalveolar lavage (BAL). Biomarkers of tissue damage were elevated to a higher extent in mice exposed to CNCP. Compared to CNCP, CNCS caused a significant increase in the accumulation of oxidatively modified proteins. The up-regulation of inflammatory cytokines was higher in the lungs after CNCS treatments. Most importantly, CNCP materials were significantly longer than CNCS. Taken together, our data suggests that particle morphology and nanosize dimensions of CNCs, regardless of the same source, may be critical factors affecting the type of innate immune inflammatory responses. Because various processes have been developed for producing highly sophisticated nanocellulose materials, detailed assessment of specific health outcomes with respect to their physical–structural–chemical properties is highly warranted.

**KEYWORDS:** Nanocellulose, Cellulose nanowhiskers, Nanofibers, Nanofiller



## INTRODUCTION

Cellulose nanowhiskers also known as nanocrystals (CNC) are a crystalline form of cellulose, the most abundant natural biopolymers on earth.<sup>1</sup> In recent years, CNC have received a great deal of attention due to their outstanding characteristics, such as nanoscale dimension, high surface area, hydrophilicity, biodegradability, increased tensile strength, and stiffness/strain.<sup>2,3</sup> CNC are typically produced by acid hydrolysis of cellulose fibers and have short needle- or rod-like shapes with lengths ranging from 100–1000 nm. The presence of a large number of chemical functionalities within the cellulose structure provides a unique platform for surface and shape modification by diverse chemistries.<sup>4</sup> Significant research efforts have been dedicated toward enhancements of the properties of CNC using various renewable sources, e.g., wood, cotton, root vegetables, straw, bacteria, and algae.<sup>5–8</sup> It was reported that the dimensions and properties of CNC vary depending on their source and hydrolysis methods employed. CNC produced from wood and cotton have a shorter length compared to those

derived from bacteria and algae.<sup>6,9–11</sup> Compared to physical properties of fibers/fibrils of native cellulose, CNC products exhibit significant improvements in electrical, optical, and magnetic features<sup>12</sup> and have a high elastic modulus.<sup>12–14</sup> Due to their enhanced physical, mechanical, and structural characteristics, CNC are considered as superior nanofiller materials compared to cellulose fibers/fibrils or other inorganic fillers. Nevertheless, the same properties of CNC used beneficially for industrial applications could be toxic and hazardous to humans. Having a high aspect ratio and stiffness, CNC could cause toxicity similar to carbonaceous fibers and/or asbestos. Therefore, it becomes critical to evaluate the potential health effects associated with exposure to CNC.

**Special Issue:** Sustainable Nanotechnology 2013

**Received:** March 4, 2014

**Revised:** April 14, 2014

**Published:** April 18, 2014

Recent evidence suggests that occupational exposure to nanocellulosic materials may be associated with pulmonary toxicity.<sup>15–21</sup> Very limited data are currently available on potential toxicity of CNC. Using human endothelial cells, Lee and his co-workers reported that CNC were nontoxic to these cells at the concentration ranges of 0–50  $\mu\text{g}/\text{mL}$ .<sup>18</sup> It has been reported that exposure of nine different aquatic species to CNC resulted in very low environmental toxicity.<sup>17</sup> Exposure of 3D cell co-cultures employed as a model of human airway epithelial barrier to CNC caused much less cytotoxicity with diminished release of inflammatory mediators as compared to carbon nanotubes or crocidolite asbestos.<sup>14</sup> While these published data suggest that CNCs were nontoxic to exposed cells, Ungvary and co-workers reported that a single intratracheal administration of microfibrillated cellulose (15 mg/rat) caused an increase in IgA level in BAL fluid, formation of fibrous bronchiolitis, and pulmonary granulomas.<sup>20</sup> Several other studies using rats and hamsters revealed that exposure to cellulose microfibrils also caused inflammation, alveolitis, granulomatous lesions, and pulmonary fibrosis.<sup>16,19–21</sup> These findings were attributed to low clearance and biopersistence of cellulose.<sup>16</sup>

The objective of this study was to evaluate whether differently processed forms of CNC (solid flake/powder, liquid, gel) derived from the same source could cause distinct pulmonary toxicity in mice. To do this, C57BL/6 mice were exposed by pharyngeal aspiration to respirable unmodified 10 wt % suspension (CNCS) and freeze-dried powder (CNCP) forms of CNC. Acute adverse effects of CNCS and CNCP were assessed by changes in markers of inflammation, pulmonary damage, and oxidative stress in mouse lungs 24 h post pharyngeal exposure.

## MATERIALS AND METHODS

**Animals.** Specific pathogen-free adult female C57BL/6 mice (7–8 week old) were supplied by Jackson Laboratories (Bar Harbor, ME). Animals were individually housed in the National Institute for Occupational Safety and Health (NIOSH) animal facilities approved by the Association for Assessment and Accreditation of Laboratory Animal Care International (AAALAC). Mice were acclimated for at least 1 week prior to use. Sterile Sani-Chip bedding (Harlan Teklad, Madison, WI) was changed weekly. Animals were supplied with water and food (Harlan Teklad, 7913, NIH-31 Modified Mouse/Rat Diet, Irradiated; Harlan Teklad, Madison, WI) *ad libitum* and housed under controlled light, temperature, and humidity conditions. All experiments were conducted under a protocol approved by the Animal Care and Use Committee of NIOSH.

**Preparation and Administration of CNC.** Wood pulp-derived cellulose nanocrystals, the unmodified 10 wt % suspension (gel form; CNCS) and freeze-dried (powder form; CNCP) samples were a gift from Forest Products Laboratory -FPL (United States Forest Service, Madison, WI). Stock suspensions of CNCS, CNCP, and asbestos (5 mg/mL) were prepared in USP grade water with pH adjusted to 7.0. The samples were sonicated for 2 min with a probe sonicator (Branson Sonifier 450, 10 W continuous outputs) and then sterilized by autoclaving. These stock suspensions were further diluted prior to animal exposures. Endotoxin levels in all used CNC samples were below the detection limit (0.01 EU/mL) as was assessed by a Limulus amoebocyte lysate (LAL) chromogenic endpoint assay kit (Hycult biotech, Inc., Plymouth Meeting, PA).

The bolus doses of CNCS, CNCP, and asbestos were given to C57BL/6 mice by pharyngeal aspiration. Briefly, after anesthetization with a mixture of ketamine and xylazine (62.5 and 2.5 mg/kg subcutaneous in the abdominal area), the mouse was placed on a board in a near vertical position and the animal's tongue extended with lined forceps. A suspension (approximately 40  $\mu\text{L}$ ) of CNCP or

CNCS (50, 100, and 200  $\mu\text{g}/\text{mouse}$ ), or crocidolite asbestos (50  $\mu\text{g}/\text{mouse}$ ) prepared in sterile USP grade water was placed posterior on the tongue, which was held until the suspension was aspirated into the lungs. Control mice were administered sterile USP grade water as a vehicle. The mice revived unassisted after approximately 30–40 min. All mice in each group survived this exposure procedure and exhibited no negative behavioral or health outcomes.

**Collection of Bronchoalveolar Lavage and Cell Counting.** Mice were sacrificed 24 h post-exposure by intraperitoneal injection of sodium pentobarbital (100 mg/kg) and exsanguinated. The trachea was cannulated with a blunted 22-gauge needle, and bronchoalveolar lavage (BAL) was performed with cold sterile  $\text{Ca}^{2+}/\text{Mg}^{2+}$ -free PBS at a volume of 0.7 mL for the first lavage (kept separate) and 0.8 mL for subsequent lavages. A total of 5 mL of bronchoalveolar lavage fluid (BALF) per mouse were collected and pooled in sterile centrifuge tubes. BAL cells were separated by centrifugation and washed in  $\text{Ca}^{2+}/\text{Mg}^{2+}$ -free PBS by alternate resuspension and centrifugation (200  $\times$  g, 10 min, 4  $^{\circ}\text{C}$ ). Cell-free first fraction BALF aliquots were used immediately or stored at 4  $^{\circ}\text{C}$  for LDH assays, while the remainder were frozen at  $-80^{\circ}\text{C}$  until analyzed for oxidative stress marker and cytokine/chemokine levels. The degree of pulmonary inflammatory response was estimated by the total cell counts, as well as alveolar macrophages, neutrophils, eosinophils, and lymphocytes recovered from the BAL fluid. Alveolar macrophages, neutrophils, eosinophils, and lymphocytes were identified in cytospin preparations stained with a Hema-3 kit (Fisher Scientific, Pittsburgh, PA) by their characteristic cell morphology, and differential counts of BAL cells were performed.

**Analysis of Cytokines/Chemokines.** Levels of cytokines/chemokines were assayed in the acellular BAL fluid using a Bio-Plex system (Bio-Rad, Hercules, CA). The concentrations of 23 different cytokines/chemokines (IL-1 $\alpha$ , IL-1 $\beta$ , IL-2, IL-3, IL-4, IL-5, IL-6, IL-9, IL-10, IL-12p40, IL-12p70, IL-13, IL-17, eotaxin, G-CSF, GM-CSF, INF- $\gamma$ , KC, MCP-1, MIP-1 $\alpha$ , MIP-1 $\beta$ , RANTES, and TNF- $\alpha$ ) were measured using a mouse cytokine group I panel 23-Plex assay kit. An aliquot of BAL fluid (50  $\mu\text{L}$  taken as is) was used for analyzing and determining the concentrations of different cytokines/chemokines. Bio-Plex Manager 6.1 software (Bio-Rad, Tokyo) was used for estimating the concentrations of cytokines/chemokines based on standard curves.

**Lactate Dehydrogenase (LDH) Activity.** The activity of LDH was assayed spectrophotometrically by monitoring the reduction of nicotinamide adenine dinucleotide at 340 nm in the presence of lactate using Lactate Dehydrogenase Reagent Set (Pointe Scientific, Inc., Lincoln Park, MI).

**Blood Smears.** Blood samples were collected from anesthetized mice via the posterior vena cava. Blood smears were stained and counted to differentiate basophils, neutrophils, lymphocytes, monocytes, and eosinophils 24 h post-exposure to CNCS and CNCP.

**Oxidative Stress Markers.** For assessment of oxidative stress in the lungs of mice exposed to CNCS, CNCP, or asbestos, measurements of 4-hydroxynonenal (4-HNE) and protein carbonyls were done in the BAL fluid. 4-HNE and protein carbonyls were measured by ELISA using the OxiSelect HNE-His adduct kit (Cell Biolabs, Inc., San Diego, CA) and Biocell PC ELISA kit (Northwest Life Science Specialties), respectively. Sensitivity of the assays was < 0.1 nmol/mg of protein.

**Particle Imaging and Size Measurements.** Transmission electron micrographs (TEM) were obtained on a JEOL TEM 1220 (Peabody, MA) at a working voltage of 80 kV. TEM images were photographed by placing a drop of diluted sample on a Formvar-coated copper grid to dry. Several TEM images were analyzed to identify at least 5–10 individual particles per image to estimate approximate dimensions of CNCS or CCNP particles.

Images of crocidolite asbestos suspensions were obtained by field emission scanning electron microscopy (SEM). In brief, asbestos particles deposited on polycarbonate filter were viewed under a field emission scanning electron microscope (model S-4800; Hitachi, Tokyo, Japan) at 400 and 30,000 magnifications. A total of 10–20 particles per image were analyzed to determine the average length and width of the asbestos fibers.

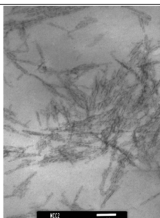
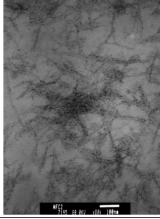
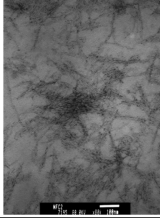
**Dynamic Light Scattering (DLS) Analysis.** The estimations of the average hydrodynamic diameter ( $Z_{\text{avg}}$ ) of CNCS or CNCP particles were carried out on a Nanotracer 252 (Microtrac, Montgomeryville, PA) using Microtrac particle sizing software, version 4.20, with a backscatter angle of  $90^\circ$  and a laser wavelength of 657.0 nm. Autoclaved and sonicated stock solutions of CNCS and CNCP (5 mg/mL particles) were suspended in ultrapure USP grade water to achieve 0.1 mg/mL samples of CNC. Refractive indexes (RI) of 1.530 for CNCS and CNCP and 1.330 for the solvent (water) at the temperature setting of  $25^\circ\text{C}$  were used as instrument parameters. The mean hydrodynamic diameters reported are averages of at least three different measurements obtained using two separate preparations of particles.

**Statistical Analysis.** Treatment-related differences compared to controls were evaluated using nonparametric Kruskal–Wallis ANOVA on Ranks followed by Dunn's test. All pairwise comparisons between individual groups (dose–response) were performed using the Holm–Sidak multiple comparison method. Statistical significance was considered at  $P < 0.05$ . Data are presented as means  $\pm$  SE.

## RESULTS

**Particle Characterization.** The structure and dimensions of CNCS and CNCP were characterized by transmission electron microscopy (TEM) and dynamic light scattering (DLS) techniques. The TEM analysis of CNCS and CNCP suspensions in USP grade water revealed presence of needle- or rod-like particle morphologies (Table 1). DLS measurements

**Table 1. Average Dimensions of Cellulose Nanocrystals (CNC)<sup>a</sup>**

Particle Type	Average Particle size		Representative Pictures
	DLS		
CNCS (10 wt% gel/suspension of CNC)	Mean length		
	1.	89.62 nm	
	2.	97.61 nm	
	3.	78.09 nm	
$Z_{\text{avg}}$ : $88.4 \pm 9.8$ nm			
TEM: $90.19 \pm 3.03$ nm			
DLS			
Mean length			
CNCP (Freeze-dried Powder of CNC)	1.	371.98 nm	
	2.	228.25 nm	
	3.	312.29 nm	
	$Z_{\text{avg}}$ : $304.2 \pm 72.2$ nm		
TEM: $207.9 \pm 49.0$ nm			

<sup>a</sup>The average size/distribution and particle morphology of CNC from unmodified gel/suspension (10 wt %; CNCS) and in powder form (CNCP) were determined using DLS and TEM measurements, respectively. The hydrodynamic diameter ( $Z_{\text{avg}}$ ) from DLS and the average length and widths estimated from TEM images were represented as mean  $\pm$  SD. The reported  $Z_{\text{avg}}$  values correspond to a mean of at least three different measurements.

were employed to study mean particle size and distribution of CNCS and CNCP. Average hydrodynamic diameters ( $Z_{\text{avg}}$ ) of  $88.4 \pm 9.8$  and  $304.2 \pm 72.2$  nm were found for CNCS and CNCP, respectively. Assessment of CNCS or CNCP dimensions from TEM images are in good agreement with length estimates from DLS measurements. The length and width measurements from TEM analysis were in the range  $90.2 \pm 3.0$  and  $7.2 \pm 2.1$  nm for CNCS and  $207.9 \pm 49.0$  and  $8.2 \pm 2.3$  nm for CNCP, respectively (Table 1). In contrast,

crocidolite asbestos fibers, as estimated by SEM, had a mean length of  $\sim 7.7 \pm 1.4$   $\mu\text{m}$  and width of  $0.4 \pm 0.1$   $\mu\text{m}$ .<sup>22,23</sup>

**Exposure to CNC Triggers Enhanced Recruitment of Inflammatory Cells to Lungs.** Mice exposed to CNC displayed an increase in the number of total cells compared to control mice: an increase of 1.44-fold, 1.40-fold, and 1.56-fold for 50, 100, and 200  $\mu\text{g}$  of CNCP per mouse, and 1.22-fold, 1.33-fold, and 1.63-fold for 50, 100, and 200  $\mu\text{g}$  of CNCS per mouse, respectively (Figure 1A). A dose-dependent increase in PMNs: 480-fold, 724-fold, and 1124-fold for CNCP and 143-fold, 453-fold, and 1084-fold for CNCS was observed compared to controls. Exposure to CNCP or CNCS (50  $\mu\text{g}$ /mouse) induced a greater number of PMNs compared to asbestos particles: approximately 480-fold and 143-fold compared to 57-fold, respectively. While CNCS induced less PMN influx compared to CNCP at the lowest dose (50  $\mu\text{g}$ /mouse), the overall increase in PMNs upon exposure to 200  $\mu\text{g}$  of CNCS and CNCP particles was similar:  $1084 \pm 66$  vs  $1124 \pm 154$  folds, respectively (Figure 1C). Furthermore, exposure to CNC also triggered an increase in the accumulation of eosinophils (Figure 1D). An increase of up to 47-fold and 181-fold in eosinophil levels was found in mice exposed to 200  $\mu\text{g}$  per mouse of CNCS and CNCP, respectively. Compared to CNCS or CNCP, exposure to a low dose of asbestos (50  $\mu\text{g}$ /mouse) caused slightly higher accumulation of eosinophil levels (48-fold vs 19-fold or 36-fold). The overall higher levels of PMNs and other inflammatory cells upon CNCS or CNCP exposure, compared to asbestos, indicates an acute inflammatory response more severe of CNC materials.

**Exposure to CNC Increases LDH Activity in BAL.** Pulmonary damage after CNCS, CNCP, and asbestos exposure was assessed by LDH enzyme activity in the BAL fluid (Figure 2A). An increase of up to 1.63-fold and 1.57-fold in LDH activity compared to the control was found in the lungs after pharyngeal aspiration with CNCS and CNCP, respectively. The LDH levels after CNC exposures were similar to asbestos (Figure 2A; 50  $\mu\text{g}$ ). These results suggest acute pulmonary cell damage in mice exposed to CNC.

**Oxidative Stress Responses Increased after Pharyngeal Aspiration Exposure to CNC.** Oxidative damage following exposure to CNCS, CNCP, and asbestos was evaluated by the presence of 4-hydroxynonenal (4-HNE) and protein carbonyl formation (Figure 2B,C). A dose-dependent increase in the accumulation of protein carbonyls was detected upon exposure to CNCP (Figure 2B). CNCP treatment caused up to 2.1-fold increase in protein carbonyl levels vs control in the lungs of exposed mice. However, the magnitude of these changes was less prominent compared to CNCS, where the increase in carbonyls was up to 2.6-fold higher compared to those observed in controls at 24 h post-exposure. In contrast to CNC, the levels of protein carbonyls in mice exposed to asbestos (50  $\mu\text{g}$ /mouse) remained similar to controls (Figure 2B). Both CNCS and CNCP caused a significant increase in 4-HNE levels compared to controls, albeit at higher concentrations (100 and 200  $\mu\text{g}$  per mouse). An increase of up to 1.7-fold and 1.9-folds (vs control) was detected in the lungs after exposure to CNCP and CNCS, respectively (Figure 2C). However, the 4-HNE levels either slightly decreased or remained similar to controls in mice exposed to 50  $\mu\text{g}$  of CNCS, CNCP, or asbestos. Overall, the magnitude of oxidative damage responses in the lungs were more pronounced in mice treated with CNC than asbestos.

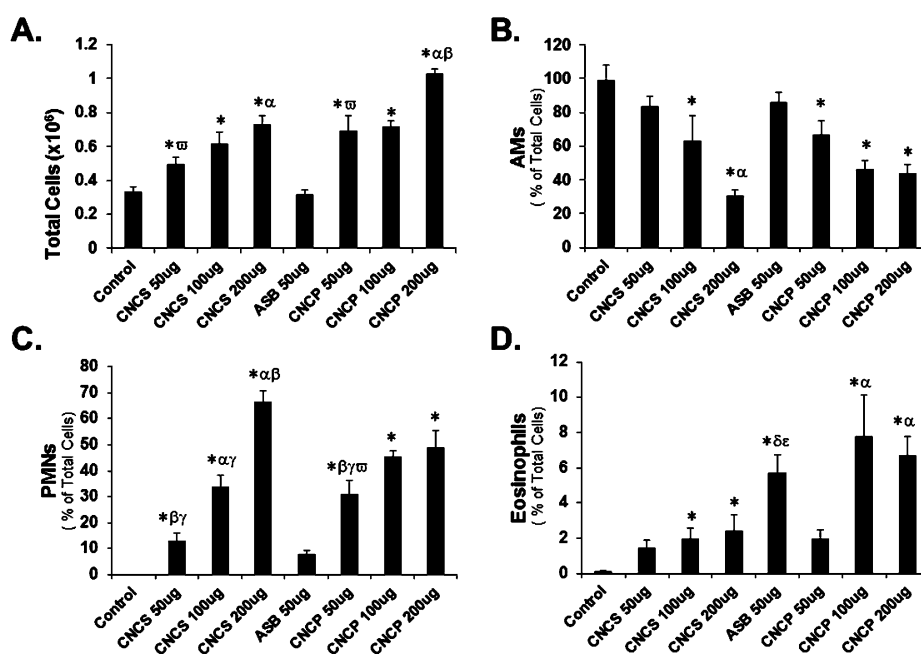


**Figure 1.** Cell profiles in BAL fluid of C57BL/6 mice 24 h post-exposure to cellulose nanocrystals or asbestos via pharyngeal aspiration. (A) Total cells, (B) alveolar macrophages (AMs), (C) polymorphonuclear leukocytes (PMNs), and (D) eosinophils. Three different doses (50, 100, and 200  $\mu\text{g}$  per mouse) were studied to understand the effects of CNC gel/suspension (CNCS) and powder form (CNCP). A single dose (50  $\mu\text{g}$ /mouse) of asbestos (ASB) was considered as a positive control in this study. Means  $\pm$  SE ( $n = 5$  mice per group).  $p < 0.05$  compared to \*control: a dose of  $^{\alpha}50$ ,  $^{\beta}100$ , or  $^{\gamma}200$   $\mu\text{g}$ /mouse of CNCS/CNCP,  $^{\alpha}50$   $\mu\text{g}$  of asbestos particles,  $^{\beta}50$   $\mu\text{g}$  of CNCP, or  $^{\epsilon}50$   $\mu\text{g}$  of CNCS particles.

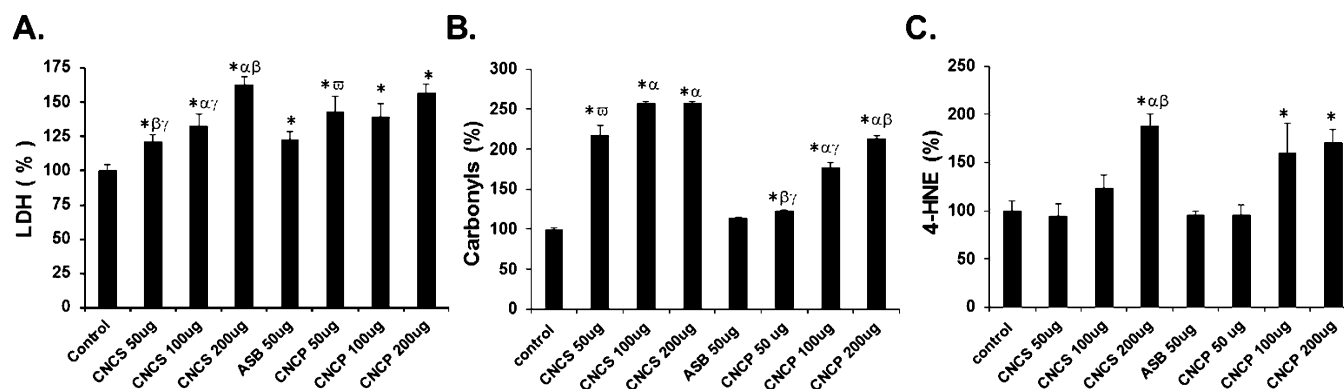


**Figure 2.** Tissue damage and oxidative stress responses in BAL fluid of C57BL/6 mice 24 h post-exposure to cellulose nanocrystals or asbestos materials via pharyngeal aspiration. (A) Lung damage as evaluated by change in lactate dehydrogenase (LDH) activity. Oxidative stress was measured as (B) formation of protein carbonyls and (C) levels of 4-hydroxynonenal (4-HNE). Two different processed forms of CNC were investigated: gel/suspension (CNCS) and a powder form (CNCP). Means  $\pm$  SE ( $n \geq 5$  mice per group).  $p < 0.05$  compared to \*control: a dose of  $^{\alpha}50$ ,  $^{\beta}100$ , or  $^{\gamma}200$   $\mu\text{g}$ /mouse of CNCS/CNCP,  $^{\alpha}50$   $\mu\text{g}$  of asbestos particles,  $^{\beta}50$   $\mu\text{g}$  of CNCP, or  $^{\epsilon}50$   $\mu\text{g}$  of CNCS particles.

**Cytokine/Chemokine Levels after Exposure to CNCS, CNCP and Asbestos.** Cytokines and chemokines are important mediators of the host defense playing a pro-inflammatory role in pulmonary inflammation during pathogen invasion. Therefore, 23 different cytokines/chemokines were measured in BAL fluids of mice exposed to CNCS and CNCP. Several cytokines and chemokines were found to be elevated in the BAL fluid of mice at 24 h post-exposure to CNCS, CNCP, or asbestos (Table 2). A comparison of up-regulated cytokines and chemokines found in the lungs of mice exposed to a high dose (200  $\mu\text{g}$ ) of CNCS and CNCP is presented in Figures 3 and 4. A total of 12 cytokines (IL-1 $\alpha$ , IL-1 $\beta$ , IL-5, IL-6, IL-12p40, G-CSF, GM-CSF, KC, MCP-1, MIP-1 $\alpha$ , MIP-1 $\beta$ , and TNF- $\alpha$ ) were significantly up-regulated compared to control mice after exposure to CNCS and CNCP (Figures 3A and 4).

These cytokines, with the exception of IL-1 $\alpha$ , IL-12p40, and TNF- $\alpha$ , were also elevated in mice exposed to asbestos (Table 2). Strikingly, the comparison of the median values of all the cytokines/chemokines suggests that exposure to CNCS (with the exception of IL-1 $\alpha$  and TNF- $\alpha$ ) caused more prominent changes (Figure 4, solid lines in the box plot). While the mean/average value of TNF- $\alpha$  was still higher after treatment with CNCS compared to CNCP; both the mean (dotted lines) and median (solid lines) values for IL-1 $\alpha$  were higher following exposure to CNCP (Figure 4). The significantly higher levels of GM-CSF, KC, MIP-1 $\alpha$ , and MIP-1 $\beta$  in the CNCS group ( $^{\alpha}p < 0.05$ ) indicates that CNCS induces stronger acute inflammatory response compared to CNCP (Figure 4). The level of IL-4, IL-10, IL-12p70, and IFN- $\gamma$  were found to be significantly elevated only after exposure to CNCS. While the up-regulation of IL-13

**Table 2. Comparison of Levels of Inflammatory Cytokines and Chemokines in BAL Fluid of C57BL/6 Mice Exposed to Cellulose Nanocrystals (CNC) and Asbestos (ASB) Particles<sup>a</sup>**

	control	CNCS (50 $\mu\text{g}$ )	CNCS (100 $\mu\text{g}$ )	CNCS (200 $\mu\text{g}$ )	ASB (50 $\mu\text{g}$ )	CNCP (50 $\mu\text{g}$ )	CNCP (100 $\mu\text{g}$ )	CNCP (200 $\mu\text{g}$ )
IL-1 $\alpha$	1.1 $\pm$ 0.1	10.3 $\pm$ 1.4*	8.8 $\pm$ 1.7*	11.4 $\pm$ 2*	1.3 $\pm$ 0.3	5.1 $\pm$ 0.8*	8.4 $\pm$ 0.5*	22.2 $\pm$ 4.7*
IL-1 $\beta$	49 $\pm$ 2.6	93.4 $\pm$ 2.4*	80.3 $\pm$ 4.3*	79.2 $\pm$ 3.7*	60 $\pm$ 4.2*	53.8 $\pm$ 4	61.1 $\pm$ 2.3*	65.2 $\pm$ 7.5*
IL-4	0.02 $\pm$ 0	1.2 $\pm$ 0.2*	1.8 $\pm$ 0.5*	1.8 $\pm$ 0.1*	ND	ND	ND	ND
IL-5	3.2 $\pm$ 0.6	13.1 $\pm$ 3.3*	33.6 $\pm$ 10.9*	26.7 $\pm$ 4.9*	26 $\pm$ 7*	9 $\pm$ 1.4*	11.4 $\pm$ 1*	10.6 $\pm$ 1.6*
IL-6	1.2 $\pm$ 0.1	61.6 $\pm$ 14*	74.1 $\pm$ 12.1*	61.9 $\pm$ 9.6*	4.6 $\pm$ 0.9*	9.1 $\pm$ 1.2*	13.3 $\pm$ 1.1*	41 $\pm$ 10.2*
IL-9	31.5 $\pm$ 6.7	48.2 $\pm$ 8.3*	34.3 $\pm$ 11.5	26.9 $\pm$ 4.2	ND	ND	ND	ND
IL-10	3.3 $\pm$ 0.6	6.4 $\pm$ 0.2*	4.3 $\pm$ 1	4.4 $\pm$ 0.3*	2.6 $\pm$ 0.7	2.3 $\pm$ 0.4	2.4 $\pm$ 0.4	4.2 $\pm$ 1
IL-12p40	126 $\pm$ 22.2	381 $\pm$ 32.3*	458.1 $\pm$ 69.9*	414 $\pm$ 48.6*	88.4 $\pm$ 13.2	256.2 $\pm$ 45.5*	411.1 $\pm$ 71.2*	314.1 $\pm$ 79.1*
IL-12p70	14.8 $\pm$ 3	48.7 $\pm$ 3.3*	33.9 $\pm$ 4.9*	37.2 $\pm$ 4.1*	8.6 $\pm$ 1	11.6 $\pm$ 2.1	10.5 $\pm$ 1.5	17.3 $\pm$ 2
IL-13	12.6 $\pm$ 0.8	12.7 $\pm$ 0.6	11.2 $\pm$ 0.7	11.4 $\pm$ 0.5	23 $\pm$ 2.5*	13.2 $\pm$ 1.4	18.0 $\pm$ 1.1*	23.7 $\pm$ 3.3*
IL-17A	2.2 $\pm$ 0.4	2.9 $\pm$ 0.5	3.5 $\pm$ 1	2.2 $\pm$ 0.3	2.5 $\pm$ 0.5	1.6 $\pm$ 0.2	1.4 $\pm$ 0.1	1.9 $\pm$ 0.2
eotaxin	295.9 $\pm$ 21	146.1 $\pm$ 25.4	109.2 $\pm$ 50.7	101.9 $\pm$ 27	327.9 $\pm$ 34	355.3 $\pm$ 44	259 $\pm$ 37.6	301 $\pm$ 31.5
G-CSF	3.4 $\pm$ 0.8	18417.7 $\pm$ 3689.8*	36979 $\pm$ 8599.1*	26718.5 $\pm$ 6736.3*	120.8 $\pm$ 39.2*	391.1 $\pm$ 79.4*	726.6 $\pm$ 51.6*	3235.8 $\pm$ 861.7*
GM-CSF	28.4 $\pm$ 2	108.2 $\pm$ 21.3*	146.7 $\pm$ 16.7*	150.7 $\pm$ 26.5*	44.5 $\pm$ 6.4*	31.5 $\pm$ 3.9	28.9 $\pm$ 2.4	71.1 $\pm$ 14.9*
IFN- $\gamma$	2.2 $\pm$ 0.5	3.7 $\pm$ 0.4*	ND	4.2 $\pm$ 0.3*	2.3 $\pm$ 0.3	2.2 $\pm$ 0.2	2.6 $\pm$ 0.3	2.7 $\pm$ 0.3
KC	3.3 $\pm$ 0.3	337.6 $\pm$ 54.3*	650.2 $\pm$ 101.7*	514.7 $\pm$ 75.3*	8.2 $\pm$ 1.2*	20 $\pm$ 2.3*	18.9 $\pm$ 3.3*	22.3 $\pm$ 5.7*
MCP-1	7.8 $\pm$ 1.2	253.3 $\pm$ 42.3*	397.5 $\pm$ 38.8*	269.8 $\pm$ 27.8*	32 $\pm$ 2.8*	46.5 $\pm$ 7.9*	101.1 $\pm$ 12.7*	290.3 $\pm$ 111.8*
MIP-1 $\alpha$	2.5 $\pm$ 0.3	65.3 $\pm$ 6.6*	69.2 $\pm$ 14.8*	58.1 $\pm$ 3.3*	7.1 $\pm$ 1.1*	17 $\pm$ 3.2*	25.5 $\pm$ 1.3*	41.7 $\pm$ 9.3*
MIP-1 $\beta$	2.0 $\pm$ 0.3	36.1 $\pm$ 2.7*	33 $\pm$ 2.1*	31 $\pm$ 1.7*	5.3 $\pm$ 0.4*	9 $\pm$ 1.6*	13.9 $\pm$ 1.1*	19.3 $\pm$ 4.6*
RANTES	1.7 $\pm$ 0.3	1.8 $\pm$ 0.2	2.2 $\pm$ 0.6	2.1 $\pm$ 0.2	1.7 $\pm$ 0.4	1.6 $\pm$ 0.2	2.3 $\pm$ 0.4	4.0 $\pm$ 0.4*
TNF- $\alpha$	19.7 $\pm$ 1	33.9 $\pm$ 3.3*	52.3 $\pm$ 6.1*	57.3 $\pm$ 3.9*	19.7 $\pm$ 1.5	25.5 $\pm$ 1*	46.2 $\pm$ 2.6*	74.7 $\pm$ 15.9*

<sup>a</sup>Mice were exposed to two forms of wood-derived CNC materials: unmodified 10 wt % CNC gel/suspension (CNCS) and a powder form (CNCP) obtained by freeze-drying. These measurements were performed using a Bio-Rad 23-plex mouse assay kit, composed of a combination of pro- and anti-inflammatory cytokines along with a subset of chemokines. The data are represented as means  $\pm$  SE and corresponds to  $\mu\text{g}/\text{mL}$  of BAL fluid. \* $p$  < 0.05 increase vs control (water treated) mice. "ND" corresponds to levels that were below detection limits of a particular cytokine/chemokine.

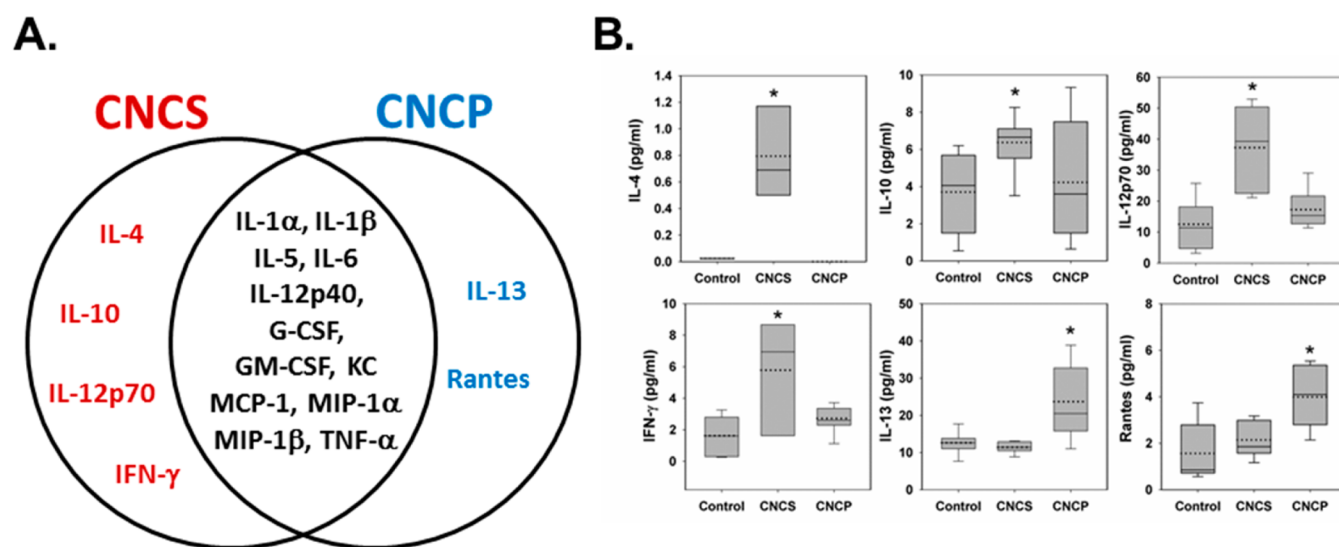


**Figure 3.** Differential responses in inflammatory mediators at 24 h post-exposure to suspension (CNCS) or powder (CNCP) form of CNC. (A) Venn diagram comparing the changes in the cytokines/chemokines levels upon 24 h post-exposure to CNCS and CNCP materials. The responses common to both groups (CNCP and CNCS) are colored in black, and those only seen after CNCP or CNCS exposure are colored in blue and red, respectively. (B) Inflammatory mediators uniquely elevated in the case of either CNCP or CNCS are shown using box plots. \* $p$  < 0.05 vs control mice.

was observed in mice exposed to CNCP or asbestos, the accumulation of chemokine (RANTES) was found to be unique to CNCP (Figure 3B, Table 2). The pattern of up-regulated cytokines/chemokines levels were less prominent in mice exposed to asbestos, with the exception of changes in IL-5 and IL-13 (Table 2). Taken together, these results suggest that CNC is a more potent inducer of acute inflammatory cytokine release compared to asbestos.

**Exposure to CNCS and CNCP Increases White Blood Cell (WBC) Counts.** Pharyngeal aspiration exposure to CNCS or CNCP (200  $\mu\text{g}/\text{mouse}$ ) caused a significant increase in WBC counts (Table 3). Compared to CNCP, a significant increase in basophil levels were found in mice exposed to CNCS (2.8 vs 3.3 folds, respectively). Therefore, assessment of WBC counts clearly indicates that exposure to CNCS or CNCP caused an acute systemic inflammation.

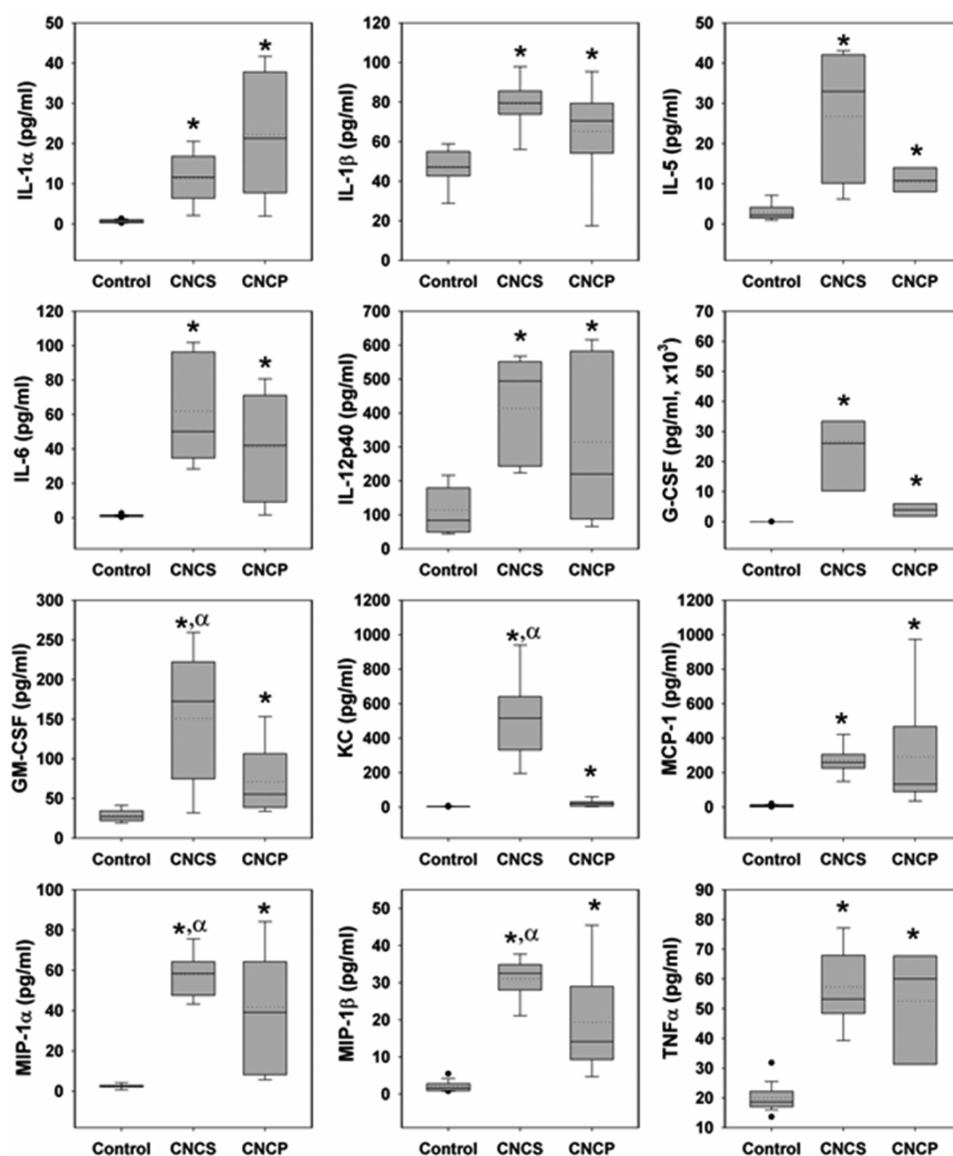


**Figure 4.** Cytokine and chemokine levels ( $\mu\text{g/mL}$ ) in the BAL fluid of mice 24 h post-exposure to cellulose nanocrystals. Box plot of the levels of inflammatory cytokines and chemokines in the BAL fluid of C57BL/6 mice ( $n = 5$ ) following aspiration of  $200 \mu\text{g}/\text{mouse}$  of unmodified gel/suspension (CNCS) or powder (CNCP) form of CNC. These measurements were performed using a Bio-Rad 23-plex mouse assay kit, composed of a combination of pro- and anti-inflammatory cytokine along with a subset of chemokines. The data are presented using box plots where the upper quartile of the box represents the 75th percentile and the lower quartile represents the 25th percentile. The dotted and solid lines inside the box correspond to mean and median values, respectively. The whiskers arising from either side of the box represent the upper and lower limits of outlier boundaries. Data points that fall outside this range are considered “outliers” and are represented as black spots/circles on the plot. \* $p < 0.05$  vs control (water treated) mice.  $^{\alpha}p < 0.05$  vs mice exposed to CNCP particles.

**Table 3. Differential Cell Counts in Blood of Mice Exposed to Suspension (CNCS) and Powder (CNCP) Forms of Cellulose Nanocrystals<sup>a</sup>**

per $2 \times 10^5$ total cells	red blood cells	basophils	PMNs	eosinophils	lymphs	total WBCs
control	$199,975.9 \pm 4.5$	$9.7 \pm 1.9$	$1.5 \pm 0.6$	$0 \pm 0$	$12.8 \pm 2$	$24 \pm 4.5$
CNCP ( $200 \mu\text{g}$ )	$199,935.7 \pm 8.8$	$26.8 \pm 0.9^*$	$11.3 \pm 1.2^*$	$3.6 \pm 0.8^*$	$22.6 \pm 6^*$	$64.3 \pm 8.9^*$
CNCS ( $200 \mu\text{g}$ )	$199,922.9 \pm 5.7$	$32.3 \pm 1.4^{*\alpha}$	$11.9 \pm 1.6^*$	$4.5 \pm 0.7^*$	$28.3 \pm 3.4^*$	$77 \pm 7.1^*$

<sup>a</sup>The relative number of each type of white blood cell (WBC) was estimated by normalizing the total cells in each case to  $2 \times 10^5$  cells. The data are presented as mean  $\pm$  SE ( $n \geq 3$ ). \* $p < 0.05$  vs control (water treated) mice.  $^{\alpha}p < 0.05$  vs mice exposed to CNCP particles.

## DISCUSSION

CNC are considered to be eco-friendly novel nanomaterials with many desirable properties broadly utilized in automotive, electronics and appliances, paper and paperboard, food

packaging, hygiene and absorbent, medical, cosmetic and pharmaceutical products.<sup>3,5,8</sup> Differences in particle physical properties, size, shape, surface area, and charge have been shown to play important roles in nanomaterial toxicity. Therefore, it becomes critical to evaluate the toxicity and

health effects of different forms/sizes CNC. The objective of this study was to compare pulmonary outcomes caused by exposure of C57BL/6 mice to two different processed forms of CNC derived from wood: CNCS (10 wt %; gel/suspension) and CNCP (powder) to asbestos.

It is well known that inhalation of toxic airborne particulates cause pulmonary inflammation. Alveolar macrophages are well known to play a critical role in the recognition, processing, and clearance of pathogens and particulates. The acute phase responses to inhaled particulates are characterized by pulmonary inflammation, associated with the recruitment and activation of phagocytic cells to remove foreign particles from the lungs. We found that bolus administration of respirable CNCS and CNCP to mice caused accelerated recruitment of neutrophils, lymphocytes, and eosinophils recovered by BAL 24 h post-exposure (Figure 1). Compared to asbestos (50  $\mu\text{g}/\text{mouse}$ ), CNCS and CNCP exposure caused a significant increase in PMNs levels. Further, exposure to CNCP, not CNCS, induced eosinophilic accumulations similar to asbestos. A concomitant increase in LDH activity further supports that treatment with CNCS and CNCP induced cytotoxicity and pulmonary damage. Overall exposure to CNCP induced a more prominent increase in total BAL cells, while treatment with CNCS caused higher oxidative stress (Figure 2). Such differences in responses could be partially due to the differences in the physical dimensions of CNCS and CNCP. DLS and TEM studies revealed an increase in the size of CNCP (up to 3.5 times) compared to CNCS (Table 1). The changes in the nanoscale dimensions of CNC were associated with the self-assembling and/or agglomeration during the lyophilization/drying process.<sup>24,25</sup> Furthermore, the acute robust pulmonary inflammation in response to CNCS and CNCP resembles outcomes observed after exposure to carbonaceous fibers.<sup>26</sup>

Acute cellular responses to airborne particulates are orchestrated by release of a number of inflammatory mediators. We found that the majority of cytokines/chemokines including IL-5, IL-6, KC, G-CSF, GM-CSF, MCP-1, MIP-1 $\alpha$ , and MIP-1 $\beta$  were up-regulated upon CNCS and CNCP exposures (Figures 3 and 4). Increased release of cytokines/chemokines is consistent with the recruitment of phagocytic cells, e.g., eosinophils, neutrophils, and monocytes/macrophages (Figure 1). The marked increase in TNF- $\alpha$  and IL-1 $\alpha$  upon CNCP exposure is further supported by the excess accumulation of AMs, PMNs, and eosinophils, key producers of pro-inflammatory cytokines (Figure 1). These two cytokines (IL-1 $\alpha$  and TNF- $\alpha$ ), acting synergistically,<sup>27</sup> are implicated in the pathogenesis of many acute and chronic noninfectious/infectious respiratory diseases.

Our data indicate that up-regulation of certain cytokines/chemokines were unique to CNCP and CNCS exposures. While the accumulation of IL-4, IL-10, IL-12p70, and IFN- $\gamma$  were specific to CNCS exposure, the up-regulation of IL-13 and RANTES were observed only after CNCP treatment (Figure 3). Most importantly, the up-regulation of IFN- $\gamma$  and IL-12p70, an active form of IL-12 that stimulates production of IFN- $\gamma$ , suggests initiation of the Th1 immune responses upon CNCS exposure. The overexpression of IFN- $\gamma$  has been associated with promoting the differentiation of Th0 into Th1 cells.<sup>28</sup> In contrast to this, the up-regulation of IL-13 and RANTES after CNCP exposure was associated with induction of the type 2 T helper cell (Th2) responses in allergic inflammation.<sup>29–31</sup> The increase in IL-13 levels upon CNCP and asbestos exposure corresponded to high accumulation of eosinophils in BAL fluid

compared to CNCS (Figure 1). Considering that IL-13 is the central mediator of allergic inflammation in many organs and tissues,<sup>31</sup> we could speculate that the up-regulation of IL-13 could play a role in the mechanism(s) of immune pulmonary inflammation in response to both asbestos and CNCP. However, further studies are needed to support this hypothesis. Taken together, our data suggest that morphology and dimensions of CNC particles, regardless of same source, may cause different toxicity and could be critical factors affecting the type of innate immune inflammatory responses in lungs.

## SUMMARY

In conclusion, the presented data clearly show that cellulose nanocrystals also known as nanowhiskers, derived from wood pulp, elicit dose-dependent oxidative stress, tissue damage, and robust inflammatory responses in the lungs. However, the extent of these responses varied significantly depending on the type of CNC material investigated: CNCS (10 wt % suspension) vs CNCP (freeze-dried powder form). Compared to CNCP, greater increases in oxidative stress markers and inflammatory mediators were found in mice exposed to CNCS. A more prominent increase in BAL cells was triggered in response to CNCP. Overall, acute phase responses caused by CNC were more prominent than those triggered by crocidolite asbestos. Finally, this study shows that even slight modifications in the production of CNC materials can result in distinct respiratory responses.

## AUTHOR INFORMATION

### Corresponding Author

\*Phone: (304) 285-6177. Fax: (304) 285-5938. E-mail: ats1@cdc.gov

### Notes

The findings and conclusions in this report are those of the authors and do not necessarily represent the views of the National Institute for Occupational Safety and Health. Mention of trade names or commercial products do not constitute endorsement or recommendation for use.

The authors declare no competing financial interest.

## ACKNOWLEDGMENTS

We thank Diane Schwegler-Berry for her help in generating the TEM images.

## REFERENCES

- (1) Siro, I.; Plackett, D. Microfibrillated cellulose and new nanocomposite materials: A review. *Cellulose* **2010**, *17* (3), 459–494.
- (2) Chinga-Carrasco, G.; Syverud, K. On the structure and oxygen transmission rate of biodegradable cellulose nanobarriers. *Nanoscale Res. Lett.* **2012**, *7*, 192.
- (3) Peng, B. L.; Dhar, N.; Liu, H. L.; Tam, K. C. Chemistry and applications of nanocrystalline cellulose and its derivatives: A nanotechnology perspective. *Can. J. Chem. Eng.* **2011**, *89* (5), 1191–1206.
- (4) Habibi, Y. Key advances in the chemical modification of nanocelluloses. *Chem. Soc. Rev.* **2014**, *43* (5), 1519–42.
- (5) Samir, M.A.S.A.; Alloin, F.; Dufresne, A. Review of recent research into cellulosic whiskers, their properties and their application in nanocomposite field. *Biomacromolecules* **2005**, *6* (2), 612–626.
- (6) Terech, P.; Chazeau, L.; Cavaille, J. Y. A small-angle scattering study of cellulose whiskers in aqueous suspensions. *Macromolecules* **1999**, *32* (6), 1872–1875.
- (7) Siqueira, G.; Bras, J.; Dufresne, A. Cellulose whiskers versus microfibrils: influence of the nature of the nanoparticle and its surface

functionalization on the thermal and mechanical properties of nanocomposites. *Biomacromolecules* **2009**, *10* (2), 425–32.

(8) Lima, M. M. D.; Borsali, R. Rodlike cellulose microcrystals: Structure, properties, and applications. *Macromol. Rapid Commun.* **2004**, *25* (7), 771–787.

(9) Grunert, M.; Winter, W. T. Nanocomposites of cellulose acetate butyrate reinforced with cellulose nanocrystals. *J. Polym. Environ.* **2002**, *10* (1–2), 27–30.

(10) Beck-Candanedo, S.; Roman, M.; Gray, D. G. Effect of reaction conditions on the properties and behavior of wood cellulose nanocrystal suspensions. *Biomacromolecules* **2005**, *6* (2), 1048–1054.

(11) Samir, M.A.S.A.; Chazeau, L.; Alloin, F.; Cavallé, J.-Y.; Dufresne, A.; Sanchez, J.-Y. POE-based nanocomposite polymer electrolytes reinforced with cellulose whiskers. *Electrochim. Acta* **2005**, *50* (19), 3897–3903.

(12) Eichhorn, S. J.; Sturcova, A. Micromechanics of Tunicate and Sugarbeet Cellulose Nanocomposites. Abstracts of Papers of the American Chemical Society, 229th National Meeting of the American Chemical Society, San Diego, CA, March 13–15, 2005, Volume 229, p U307.

(13) Sturcova, A.; Apperley, D. C.; Kalaskar, D.; Eichhorn, S. J.; Jarvis, M. C. Relationship between the Micromorphology and Mechanical Properties of Cellulose. Abstracts of Papers of the American Chemical Society, 229th National Meeting of the American Chemical Society, San Diego, CA, March 13–15, 2005, Volume 229, p U286.

(14) Clift, M. J. D. Investigating the interaction of cellulose nanofibers derived from cotton with a sophisticated 3D human lung cell coculture. *Biomacromolecules* **2011**, *12* (10), 3666–3673.

(15) Adamis, Z. In vitro and in vivo assessment of the pulmonary toxicity of cellulose. *J. Appl. Toxicol.* **1997**, *17* (2), 137–141.

(16) Cullen, R. T. Tumorigenicity of cellulose fibers injected into the rat peritoneal cavity. *Inhalation Toxicol.* **2002**, *14* (7), 685–703.

(17) Kovacs, T. An ecotoxicological characterization of nanocrystalline cellulose (NCC). *Nanotoxicology* **2010**, *4* (3), 255–270.

(18) Roman, M.; Dong, S.; Hirani, A.; Lee, Y. W. Cellulose Nanocrystals for Drug Delivery. *Polysaccharide Materials: Performance by Design*; Edgar, K. J., Heinze, T., Buchanan, C. M., Eds.; ACS Symposium Series 1017; American Chemical Society: Washington, DC, 2009; pp 81–91.

(19) Tatrai, E. Role of cellulose in wood dust-induced fibrosing alveo-bronchiolitis in rat. *J. Appl. Toxicol.* **1995**, *15* (1), 45–8.

(20) Tatrai, E. In vivo pulmonary toxicity of cellulose in rats. *J. Appl. Toxicol.* **1996**, *16* (2), 129–35.

(21) Warheit, D. B., et al. Two-Week Inhalation Study in Rats with Cellulose Fibers. *Advances in the Prevention of Occupational Respiratory Diseases*; Chiyotani, K., Hosoda, Y., Eds.; International Congress Series 1153; Excerpta Medica: Amsterdam, 1998; pp 579–582.

(22) Murray, A. R.; Cassee, F. R. Factoring-in agglomeration of carbon nanotubes and nanofibers for better prediction of their toxicity versus asbestos. *Part. Fibre Toxicol.* **2012**, *9*, 10.

(23) Shvedova, A. A. Long-term effects of carbon containing engineered nanomaterials and asbestos in the lung: one year postexposure comparisons. *Am. J. Physiol.: Lung Cell. Mol. Physiol.* **2014**, *306* (2), L170–82.

(24) Han, J. Q. Self-assembling behavior of cellulose nanoparticles during freeze-drying: Effect of suspension concentration, particle size, crystal structure, and surface charge. *Biomacromolecules* **2013**, *14* (5), 1529–1540.

(25) Peng, Y. Influence of drying method on the surface energy of cellulose nanofibrils determined by inverse gas chromatography. *J. Colloid Interface Sci.* **2013**, *405*, 85–95.

(26) Murray, A. R. Factoring-in agglomeration of carbon nanotubes and nanofibers for better prediction of their toxicity versus asbestos. *Part. Fibre Toxicol.* **2012**, *9*, 10.

(27) Dinarello, C. A. Proinflammatory cytokines. *Chest* **2000**, *118* (2), 503–508.

(28) Hamza, T.; Barnett, J. B.; Li, B. Y. Interleukin 12 a key immunoregulatory cytokine in infection applications. *Int. J. Mol. Sci.* **2010**, *11* (3), 789–806.

(29) Koya, T. RANTES (CCL5) regulates airway responsiveness after repeated allergen challenge. *Am. J. Respir. Cell Mol. Biol.* **2006**, *35* (2), 147–54.

(30) Venkayya, R. The Th2 lymphocyte products IL-4 and IL-13 rapidly induce airway hyperresponsiveness through direct effects on resident airway cells. *Am. J. Respir. Cell Mol. Biol.* **2002**, *26* (2), 202–208.

(31) Wills-Karp, M. Interleukin-13: Central mediator of allergic asthma. *Science* **1998**, *282* (5397), 2258–2261.